

# Direct roles of the signaling kinase RSK2 in Cdc25C activation during *Xenopus* oocyte maturation

Ruoning Wang<sup>a,b,1</sup>, Sung Yun Jung<sup>c</sup>, Chuan Fen Wu<sup>a</sup>, Jun Qin<sup>c</sup>, Ryuji Kobayashi<sup>d</sup>, Gary E. Gallick<sup>e</sup>, and Jian Kuang<sup>a,b,2</sup>

Departments of <sup>a</sup>Experimental Therapeutics, <sup>b</sup>Molecular Pathology, and <sup>c</sup>Genitourinary Medical Oncology, University of Texas M. D. Anderson Cancer Center, Houston, TX 77030; <sup>b</sup>Program in Genes and Development, University of Texas Graduate School of Biomedical Sciences, Houston, TX 77030; and <sup>d</sup>Department of Biochemistry, Baylor College of Medicine, Houston, TX 77030

Edited\* by John Gerhart, University of California, Berkeley, CA, and approved October 6, 2010 (received for review March 22, 2010)

**The induction of M phase in eukaryotic cell cycles requires robust activation of Cdc2/cyclin B by Cdc25, which itself is robustly activated by serine/threonine phosphorylations. Although multiple protein kinases that directly activate Cdc25C have been identified, whether the combination of different primary phosphorylations of Cdc25C is sufficient to fully activate Cdc25C has not been determined. By analyzing the GST-Cdc25C phosphorylating activity in *Xenopus* egg extracts, we previously defined roles of MAPK and Cdc2/cyclin B in partially activating Cdc25C and predicted the presence of another major Cdc25C-activating kinase. In this study, we demonstrate that this missing kinase is RSK2, which phosphorylates three sites in Cdc25C and also partially activates Cdc25C. However, the phosphorylations catalyzed by MAPK, Cdc2, and RSK2 fail to fully activate Cdc25C, suggesting that additional biochemical events are required to fully activate this key cell cycle regulator.**

Cdc25C activators | p90RSK | substrate | phosphorylation sites | Cdk1 regulation

Induction of mitosis and meiosis (M phase) in the eukaryotic cell cycle requires activation of the M-Cdk complex (Cdc2/cyclin B) by the protein phosphatase Cdc25 (1, 2). At onset of M phase, Cdc25C activity increases 10- to 20-fold due to extensive phosphorylation of its N-terminal regulatory domain, and the phosphorylation increases the apparent molecular weight of Cdc25C by 20–40 kDa (3–5). In the widely accepted model for Cdc25C activation, a non-Cdc2 kinase (such as a polo-like kinase) is activated before Cdc2 activation, contributing to the initiation of Cdc25C activation. The catalytic amount of activated Cdc25C then activates a small amount of Cdc2/cyclin B, which in turn activates more Cdc25C and vice versa. This direct positive feedback loop produces concurrent and switch-like activation of Cdc2/cyclin B and the dramatic gel mobility shift of Cdc25C, indicative of Cdc25C full activation (6, 7).

Although the above model is consistent with the “all or none” characteristics of M-phase induction and the autocatalytic nature of maturation-promoting factor (MPF) and Cdc2/cyclin B in *Xenopus* oocytes (7–9), several studies have suggested that Cdc25C activation is much more complicated. For example, addition of recombinant Cdc25C to immature *Xenopus* oocyte extracts induced activation of endogenous Cdc2 and Plx1 but failed to induce the dramatic gel mobility shift of Cdc25C. The latter could, however, be induced if the phosphatase inhibitor okadaic acid (OA) was also added to oocyte extracts (10). In interphase-arrested *Xenopus* egg extracts depleted of cyclin B, the large mobility shift of Cdc25C could be induced by the phosphatase inhibitor microcystin plus the classical MPF extraction buffer (11) even in the absence of Cdc2 and Cdk2 proteins (12). These results suggest a model whereby full activation of Cdc25C involves mechanistically distinct phosphorylation steps.

To understand the complex process of Cdc25C activation during G2/M transition, our strategy has been to identify all major kinases in M phase-arrested *Xenopus* egg extracts (MEE) that phosphorylate and activate GST-tagged *Xenopus* Cdc25C (GST-Cdc25C). As GST-Cdc25C is unphosphorylated, we term the

phosphorylations catalyzed by such identified kinases “primary phosphorylations.” By fractionation of MEE, our previous results demonstrated that 10–20% of the primary Cdc25C phosphorylating activity is due to Cdc2/cyclin B, which phosphorylates Cdc25C at the proline-directed sites T138, S285, and T308 and activates GST-Cdc25C two- to fourfold. Approximately 40% of the activity is due to p42 MAPK, which phosphorylates Cdc25C at the proline-directed sites T48, T138, and S205 and also activates GST-Cdc25C two- to fourfold. The remaining activity is mainly due to an undetermined kinase of ~200 kDa by gel filtration (kinase X). However, none of the three kinases induces a dramatic gel mobility shift in GST-Cdc25C although phospho-defective mutation of the three MAPK sites (T48/T138/S205) in Cdc25C eliminates the ability of Cdc25C to undergo a dramatic gel mobility shift in progesterone-matured *Xenopus* oocytes (13). These results predicted that the large mobility shift of Cdc25C is due to the phosphorylations that require priming phosphorylations, which we term “secondary phosphorylations.” The association of the dramatic gel mobility shift of Cdc25C with the secondary phosphorylations is also demonstrated by our recent study using cell-free systems (14). To determine the role of primary phosphorylations in Cdc25C activation, we initiated this study to identify the kinase X and map its phosphorylation sites in Cdc25C. We also examined the collective effects of Cdc2, MAPK, and RSK2 on GST-Cdc25C activation.

## Results

**Kinase X Plays a Distinct Role in Cdc25C Phosphorylation.** In our previous studies (13), we fractionated the 40% ammonium sulfate precipitate of MEE by consecutive gel filtration and Q-Sepharose chromatography and followed the Cdc25C phosphorylating activity (Fig. 1A). From the Q-Sepharose chromatography, the flow-through fraction contained a Cdc2-dependent minor activity, whereas the 0.2 M NaCl eluate (QE1) contained most of the recovered activity. Further fractionation of QE1 led to the identification of MAPK as a Cdc25C activating kinase. However, immunodepletion of MAPK from QE1 removed only ~50% of the GST-Cdc25C phosphorylating activity. Whereas untreated or mock-depleted QE1 phosphorylated nine cleavage products of GST-Cdc25C of 30–76 kDa, the MAPK-depleted QE1 phosphorylated only one cleavage product of GST-Cdc25C of 76 kDa (Fig. 1B). Furthermore, when thiophosphorylated QE1 was fractionated sequentially by heparin-Sepharose chromatography and Superose 6 gel filtration, and partially cleaved GST-Cdc25C was

Author contributions: R.W., S.Y.J., J.Q., R.K., and J.K. designed research; R.W., S.Y.J., C.F.W., and R.K. performed research; R.W. contributed new reagents/analytic tools; R.W., S.Y.J., C.F.W., J.Q., R.K., G.E.G., and J.K. analyzed data; and R.W., G.E.G., and J.K. wrote the paper.

The authors declare no conflict of interest.

\*This Direct Submission article had a prearranged editor.

<sup>1</sup>Present address: Department of Immunology, St. Jude Children’s Research Hospital, Memphis, TN 92105.

<sup>2</sup>To whom correspondence should be addressed. E-mail: jkuang@mdanderson.org.

This article contains supporting information online at [www.pnas.org/lookup/suppl/doi:10.1073/pnas.1003528107/-DCSupplemental](http://www.pnas.org/lookup/suppl/doi:10.1073/pnas.1003528107/-DCSupplemental).

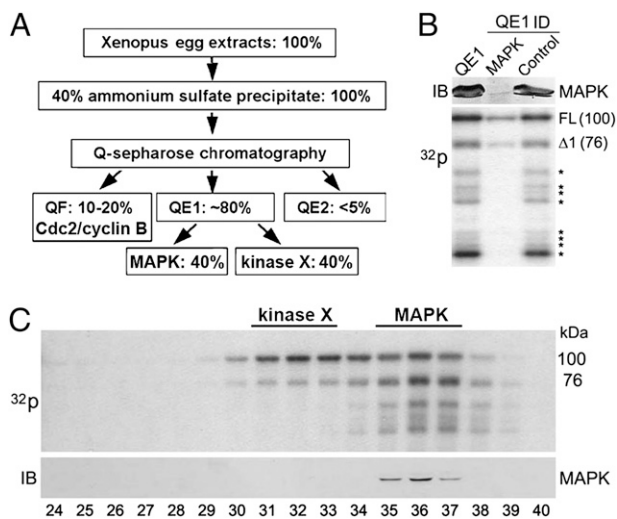


**Fig. 1.** Kinase X plays a distinct role in Cdc25C phosphorylation. (A) A schematic of biochemical fractionations of MEE and recovery of Cdc25C-phosphorylating activities. (B) After QE1 was immunodepleted (ID) with control or anti-MAPK antibodies, samples were immunoblotted with anti-MAPK antibodies and assayed for catalyzing <sup>32</sup>P incorporation of GST-Cdc25C. (C) The 0.25 M NaCl eluate from heparin-Sepharose chromatography of thiophosphorylated QE1 was fractionated by Superose 6 gel filtration, and the indicated fractions were assayed for catalyzing <sup>32</sup>P incorporation of GST-Cdc25C and immunoblotted with anti-MAPK antibodies.

phosphorylated with individual fractions, two peaks of the Cdc25C phosphorylating activity were recovered (Fig. 1C). One activity copurified with MAPK and phosphorylated GST-Cdc25C as did QE1, and the other activity (100–200 kDa) phosphorylated GST-Cdc25C similarly as did MAPK-depleted QE1. These results demonstrate that kinase X phosphorylates distinct sites in Cdc25C.

**Kinase X Is RSK2.** To identify kinase X, we fractionated MEE by consecutive steps as diagrammed in Fig. 2A. In the last step (sucrose gradient centrifugation), fractions 6 and 7 contained both the peak Cdc25C phosphorylating activity and a protein of ~90 kDa that is able to incorporate <sup>32</sup>P (Fig. 2B, *Top and Middle*). Thus proteins were separated by SDS/PAGE and silver-stained (Fig. S1A), and the visualized proteins in the sixth fraction were identified by mass spectrometry. RSK2 not only was identified by this strategy (Fig. S1B), but also peaked in fractions 6 and 7 by immunoblotting (Fig. 2B, *Bottom*), making RSK2 a strong candidate.

To determine if RSK2 is the kinase X, we produced GST-tagged N (9-205) and C (204-550) fragments of Cdc25C and phosphorylated the two proteins with fractions from the Superose 6 gel filtration, which contains both MAPK and kinase X (Fig. 2A). Whereas MAPK fractions specifically phosphorylated Cdc25C-N as anticipated, the kinase X fractions specifically phosphorylated Cdc25C-C (Fig. 2C). We then immunodepleted RSK2 or MAPK from QE1. RSK2 depletion specifically removed the Cdc25C-C phosphorylating activity, whereas MAPK depletion specifically removed the Cdc25C-N phosphorylating activity. In contrast, depletion of the residual Cdc2 by p13-Sepharose did not affect either activity (Fig. 2D). Furthermore, we phosphorylated Cdc25C-N and Cdc25C-C with a constitutively active murine RSK2 (CA-RSK) (Fig. S1C) and observed specific phosphorylation of Cdc25C-C by CA-RSK (Fig. 2E). These results demonstrate that RSK2 is the kinase X.

**RSK2 Phosphorylates Cdc25C at Amino Acids 317–319 in Vitro.** The minimal sequence requirement for phosphorylation by RSK1/2 appears to be an R/K-XX-S/T motif (15), making S287, S317,

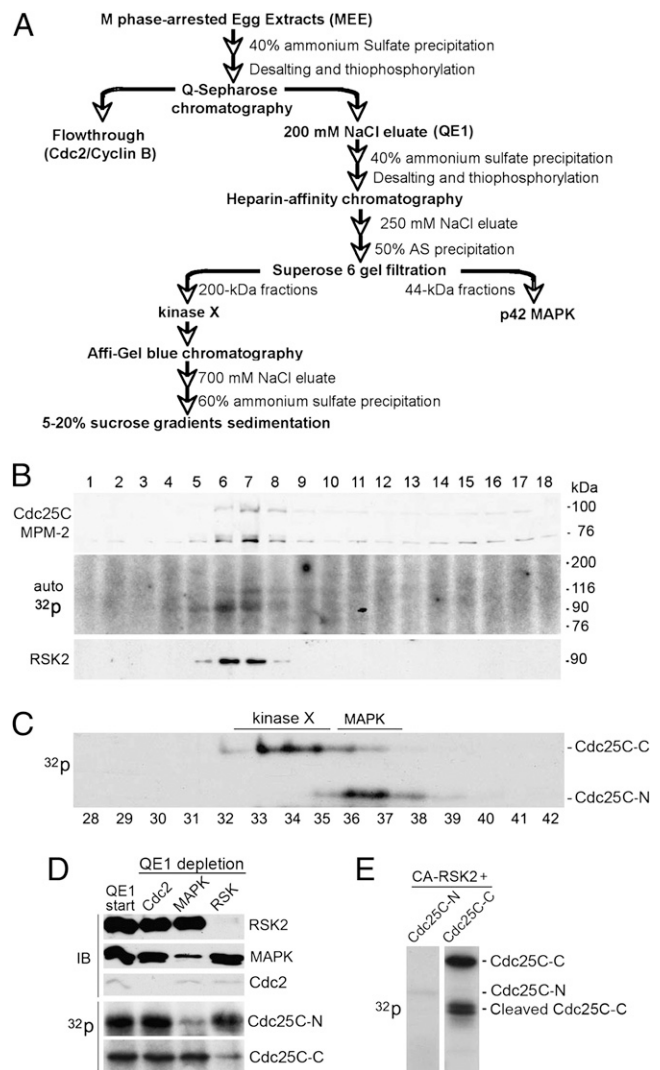


**Fig. 2.** Kinase X is RSK2. (A) Consecutive steps in purification of kinase X from MEE. (B) The sucrose gradient fractions were incubated with GST-Cdc25C and immunoblotted with the phospho-specific antibody MPM-2 (*Top*) and assayed for autophosphorylation by <sup>32</sup>P incorporation (*Middle*) and for RSK2 protein by immunoblotting with anti-RSK2 antibodies (*Bottom*). (C) Fractions from the Superose 6 gel filtration were assayed for phosphorylation of GST-Cdc25C-N and GST-Cdc25C-C by <sup>32</sup>P incorporation. (D) After QE1 was depleted of Cdc2 with p13-Sepharose, of MAPK with anti-MAPK antibodies, or of RSK2 with anti-RSK1/2 antibodies, starting material and depleted samples were immunoblotted (IB) with antibodies for each of the indicated kinases and assayed for catalyzing <sup>32</sup>P incorporation of GST-Cdc25C-N and GST-Cdc25C-C. (E) CA-RSK was assayed for catalyzing <sup>32</sup>P incorporation of GST-Cdc25C-N and GST-Cdc25C-C.

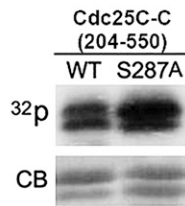
T318, S319, S336, S337, S343, T529, and T533 in Cdc25C-C potential RSK2 phosphorylation sites (Fig. 3A). Although S287 was previously reported to be phosphorylated by RSK1 in vitro (16), the S287A mutation did not decrease the phosphorylation of Cdc25C-C by CA-RSK (Fig. 3B), predicting the existence of additional RSK2 phosphorylation sites. To identify these sites, we produced different fragments of Cdc25C-C and phosphorylated them with CA-RSK. The 251–353 fragment was phosphorylated as efficiently as Cdc25C-C (Fig. 3C), whereas phosphorylation of the 499–550 fragment was barely detectable (Fig. 3D). Within the 251–353 region, the 278–308 fragment was phosphorylated in an S287-dependent manner (Fig. 3E); however, the 300–349 fragment was phosphorylated more efficiently than the 278–308 fragment (Fig. 3F). Together, these results

A

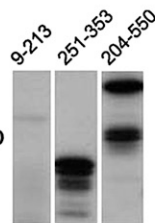
## \*Potential RSK phosphorylation sites in Cdc25C-C

191 DISLDEDCEMNLLGSPISADPPCLDGAHDDIKMQLDGFADFFSVDEEEMENPPGAVGNL 250  
 251 SSSMAILLSGPLLNDIEVSNVNNISLNRSLYRSPSMPEKLDREMLKRPVRLDSETPV 310  
 311 RVKRRRSTSSSLQPQEEFQPPRRGTSLKKTLSLCDVDISTVL 370  
 371 ALPTVTGRHQDLRYITGETLAALIHGDFSSSLVEKIFIIDCRYPEYDGGHIKGAALNLRQ 430  
 431 EEVTDYFLKQPLTPTMAQRLLIIIFHCEFSSERGPKMCRLFREEDRARNEYPSLYYPELY 490  
 491 LLKGGYKDFPEYKELCEPQSYCPMHHQDFREELKFR<sup>T529</sup>T<sup>S33</sup>T<sup>S33</sup>K<sup>\*</sup>KT<sup>\*</sup>SVGDRKRREQIARIMKL 550

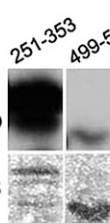
B



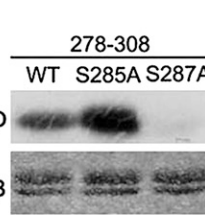
C



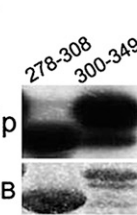
D



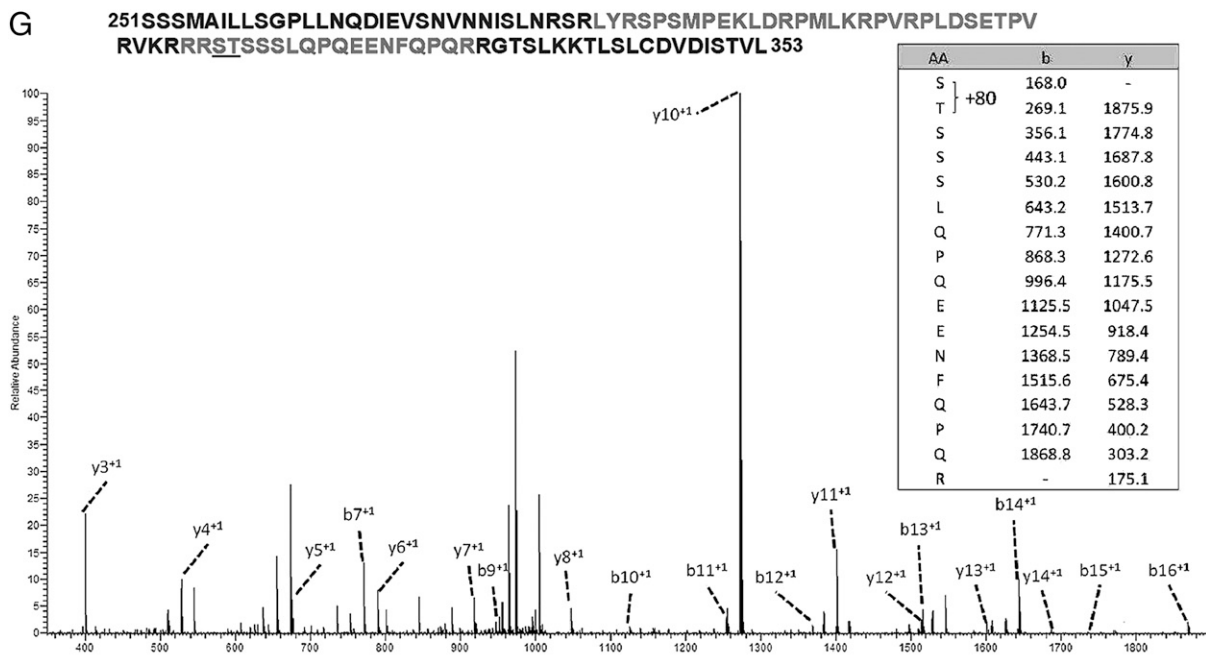
E



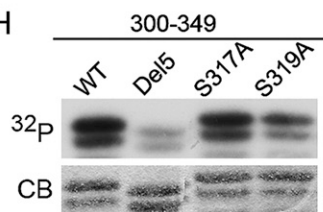
F



G



H



I

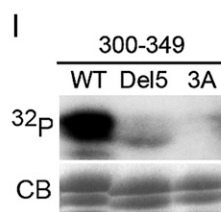


**Fig. 3.** CA-RSK phosphorylates 317–319 in Cdc25C in vitro. (A) Protein sequence of Cdc25C-C with nine R/KXXS/T motifs indicated. (B–F) Indicated GST-tagged fragments of Cdc25C were phosphorylated with CA-RSK in the presence of  $^{32}\text{P}$ - $\gamma$ -ATP, and SDS/PAGE-separated proteins were stained with Coomassie blue (CB) and subjected to autoradiography. (G) After the GST-tagged 251–353 fragment of Cdc25C was phosphorylated by CA-RSK, two tryptic peptides (282–310 and 315–333) were analyzed by nano-HPLC/MS/MS, and two phosphorylation sites (S317 and T318) were identified in one of the peptides. (H and I) Indicated forms of the GST-tagged 300–349 fragment of Cdc25C were phosphorylated with CA-RSK in the presence of  $^{32}\text{P}$ - $\gamma$ -ATP, and SDS/PAGE-separated proteins were stained with Coomassie blue (CB) and subjected to autoradiography.

demonstrate that RSK2 primarily phosphorylates the 300–349 region in Cdc25C.

The 300–349 region of Cdc25C contains six candidate RSK2 phosphorylation sites. To determine which of these six sites are phosphorylated by RSK2, we analyzed the phosphorylated residues in the CA-RSK-phosphorylated 251–353 fragment by nano-

HPLC/MS/MS. Phosphorylated S317 and T318 were detected by this approach (Fig. 3G). In parallel, we mutated different candidate RSK2 sites in the 300–349 fragment and phosphorylated the mutant peptides with CA-RSK. Although S319 phosphorylation was not detected by mass spectrometry, the S319A mutation decreased the phosphorylation. Both the 317–321 deletion

or the S317A-T318A-S319A triple mutation (3A mutation) eliminated most of the phosphorylation (Fig. 3 *H* and *I*). These results demonstrate that RSK2 primarily phosphorylates S317, T318, and/or S319 (317-319) in Cdc25C.

**RSK2 Phosphorylates Cdc25C at 317–319 in *Xenopus* Oocytes.** A commercial antibody, termed “anti-pSTS antibody” in this report, recognizes a wide range of AKT-phosphorylated proteins and some RSK-phosphorylated proteins (17, 18). When the GST-tagged Cdc25C, Cdc25C-C, and the 251–351 fragment were phosphorylated with MAPK, CA-RSK2, or MEE, the anti-pSTS antibody recognized all three proteins that had been phosphorylated by CA-RSK or MEE but none of the MAPK-phosphorylated proteins (Fig. 4*A*). Moreover, the MEE-generated immunoreactivity was dramatically decreased by the RSK inhibitor SL0101 (Fig. 4*B*), and the CA-RSK-generated immunoreactivity was eliminated by mutation of S317-T318-S319 to three alanines (Fig. 4*C*). In contrast, the individual S317A or S319A mutation did not decrease the immunoreactivity (Fig. 4*D*). Double mutations of S317A-T318A or S317A-S319A even increased the immunoreactivity, suggesting that either phosphorylation of two or more sites interferes with the Ab detection or the antibody recognizes phosphorylated T318 and/or S319 with higher affinity than phosphorylated S317. Regardless, these results demonstrate that the anti-pSTS antibody at least recognizes Cdc25C that is phosphorylated at T318 and/or S319.

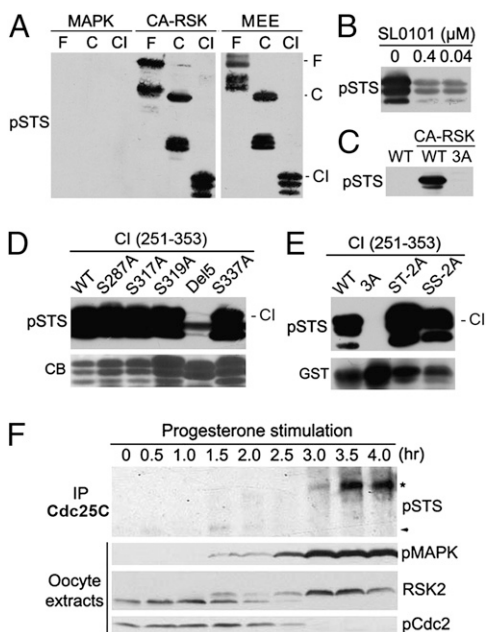


**Fig. 4.** RSK2 phosphorylates Cdc25C at 317–319 in *Xenopus* oocytes. (*A*) Indicated GST-tagged fragments of Cdc25C were phosphorylated with MAPK, CA-RSK, or MEE and immunoblotted with the anti-pSTS antibody. (*B*) GST-Cdc25C was incubated with MEE supplemented with indicated concentrations of SL0101 and immunoblotted with the anti-pSTS antibody. (*C*) The wild type (WT) and 3A mutant GST-Cdc25C-C were phosphorylated with CA-RSK and then immunoblotted with the anti-pSTS antibody. (*D* and *E*) Indicated forms of the GST-tagged 251–353 fragment of Cdc25C were phosphorylated with CA-RSK, and SDS/PAGE-separated proteins were immunoblotted with the anti-pSTS antibody and either stained with CB (*D*) or immunoblotted with anti-GST antibodies (*E*). “ST-2A” indicates mutation of S317 and T318 to 2A; “SS-2A” indicates mutation of S317 and S319 to 2A. (*F*) Extracts of *Xenopus* oocytes collected at the indicated hours after progesterone stimulation were immunoblotted for each of the indicated proteins, and Cdc25C immunoprecipitates were immunoblotted with the anti-pSTS antibody. The asterisk and arrowhead indicate shifted and nonshifted proteins, respectively.

To determine whether RSK2 phosphorylates Cdc25C at 317–319 in *Xenopus* oocytes, we immunoprecipitated Cdc25C from extracts of *Xenopus* oocytes collected at different time points after progesterone stimulation. As shown in Fig. 4*F*, the anti-pSTS antibody recognized the hyperphosphorylated Cdc25C at ~116 kDa, which correlated with a gel shift of RSK2, an indication of RSK2 activation. In addition, we induced *Xenopus* oocyte maturation by ectopic expression of a constitutively active Cdc2 (Cdc2-AF) in the presence or absence of the RSK1/2 inhibitor SL0101 or the MEK inhibitor UO126, which inhibits the activation of MAPK and its downstream kinase RSK2. Both inhibitors eliminated the immunoreactivity of Cdc25C to the anti-pSTS antibody (Fig. S2). These results demonstrate that RSK2 phosphorylates Cdc25C at 317–319 in *Xenopus* oocytes.

**RSK2 Activates Cdc25C.** To determine whether RSK2 activates Cdc25C in vitro, we phosphorylated His-Cdc25C in vitro with CA-RSK and measured Cdc25C’s phosphatase activity toward 3-O-methylfluorescein phosphate (OMFP) (19). Phosphorylation of the wild-type but not the 3A mutant form of His-Cdc25C increased Cdc25C’s phosphatase activity by 1.8- or 2.5-fold in two different experiments (Fig. 5*A* and Fig. S3), which is comparable to increases observed by MAPK-mediated phosphorylation of His-Cdc25C (13). These results demonstrate that RSK2 activates Cdc25C in vitro.

To determine whether RSK2 activates Cdc25C in vivo, we ectopically expressed the wild-type or the 3A mutant form of myc-Cdc25C in *Xenopus* oocytes and observed the kinetics of oocyte maturation. As shown in Fig. 5*B*, oocytes expressing the wild-type myc-Cdc25C matured faster than oocytes expressing the mutant protein. In addition, because ectopic expression of both myc-Cdc25C and Myr-RSK, an avian RSK that is constitutively active due to addition of the Src myristoylation sequence (20), induced oocyte maturation faster than expression of either Myc-Cdc25C or Myr-RSK (Fig. S4), we also coexpressed the wild-type or 3A mutant form of myc-Cdc25C with Myr-RSK in *Xenopus* oocytes and observed the kinetics of oocyte maturation. Again, oocytes expressing the wild-type myc-Cdc25C matured faster than oocytes expressing the mutant protein (Fig. 5*C*). These results demonstrate that RSK2 activates Cdc25C in vivo.

**Phosphorylations by MAPK, Cdc2, and RSK2 Do Not Yield Fully Activated Cdc25C.** To determine the role of different primary phosphorylations of Cdc25C in Cdc25C activation, we phosphorylated GST-Cdc25C with MEE or different combinations of MAPK, Cdc2, and RSK2 and examined their effects on the ability of GST-Cdc25C to activate Cdc2/cyclin B as diagrammed in Fig. S5. As reported previously (13), GST-Cdc25C that had been phosphorylated with Cdc25C-depleted MEE was equivalent to the activity of nonphosphorylated GST-Cdc25C at a 16-fold dilution (Fig. 6*A*), indicative of a 16-fold activation of GST-Cdc25C by MEE. However, GST-Cdc25C that had been phosphorylated by the combination of MAPK, Cdc2, and RSK2 reached the basal activity of nonphosphorylated GST-Cdc25C at a fourfold dilution. A twofold dilution of the 3-kinase mixture did not reduce its ability to activate GST-Cdc25C. The results with individual kinases or paired kinases were similar (Fig. 6*B*). These results demonstrate that primary phosphorylations induced by MAPK, Cdc2, and RSK2 fail to fully activate Cdc25C.

## Discussion

In this study, we have completed our long-term efforts to characterize all major kinases in *Xenopus* egg extracts that directly phosphorylate and activate GST-Cdc25C and have identified RSK2 as another major Cdc25C-activating kinase. This has allowed us to determine the role of different primary phosphorylations of Cdc25C in Cdc25C activation. Our results show that RSK2 phosphorylates Cdc25C at three sites that are distinct from those phosphorylated

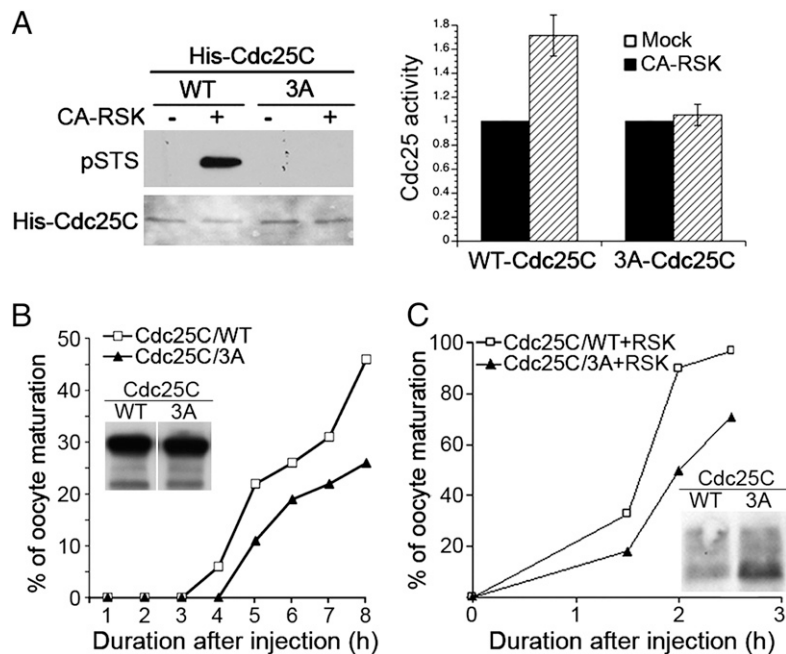


**Fig. 5.** RSK2 activates Cdc25C. (A) After the wild-type or the 3A mutant form of His-Cdc25C was mock-treated or phosphorylated with CA-RSK, the end products were immunoblotted with the anti-pSTS antibody and the anti-Cdc25C antibody (Left) or assayed for dephosphorylation of the fluorescent substrate OMFP (Right). (B) *Xenopus* oocytes were injected with mRNA for the wild type (WT) or the 3A mutant form of myc-Cdc25C, and the percentage of oocytes matured was determined at the indicated hours after the injection. Extracts of oocytes collected at the last time point were immunoblotted with anti-myc antibodies. (C) *Xenopus* oocytes were injected with mRNAs for Myr-RSK plus the wild type (WT) or the 3A mutant form of myc-Cdc25C, and the percentage of oocytes matured was determined at the indicated hours after the injection. Extracts of oocytes collected at the last time point after the injection were immunoblotted with anti-myc antibodies.

by Cdc2 and MAPK but activates Cdc25C as efficiently as these previously identified enzymes. However, although *Xenopus* egg extracts activate GST-Cdc25C 16-fold, phosphorylations of GST-

Cdc25C by MAPK, Cdc2, and RSK2, either individually or collectively, activate GST-Cdc25C only two- to fourfold. These results indicate that different primary phosphorylations do not function additively to fully activate Cdc25C.

Because different primary phosphorylations of Cdc25C by MAPK, Cdc2, and RSK2 do not work additively to achieve the full activation of Cdc25C, another plausible explanation is that the different primary phosphorylations are alternative ways of generating partially activated or primed Cdc25C, which somehow triggers the biochemical event responsible for the full activation of Cdc25C. If this model is correct, sufficient activation of any one of the three identified kinases should be able to trigger a delayed full activation of Cdc25C in progesterone-stimulated *Xenopus* oocytes if the noninhibited kinases carry enough activities. Interestingly, previous observations by us and others are largely consistent with these predictions. For example, when introduced at high levels, cyclin B, thiophosphorylated MAPK, mutant Cdc2 that cannot be phosphorylated by Wee1/Myt 1 (Cdc2-AF), and constitutively active RSK2 are each able to induce the full activation of Cdc25C and the resultant G2/M transition in *Xenopus* oocytes although after a substantial delay (13, 21, 22). On the other hand, neither inhibition of the initial cyclin B-dependent Cdc2 activation nor inhibition of the initial mos-dependent MAPK and RSK activations blocked progesterone-induced *Xenopus* oocyte maturation. Only when both mos and cyclin B syntheses were inhibited was progesterone-induced *Xenopus* oocyte maturation blocked (23).

At this stage of our thinking, the best candidate biochemical event that precipitates the full activation of Cdc25C is the secondary phosphorylation of Cdc25C that produces the dramatic gel mobility shift of Cdc25C. The phosphorylation-dependent dramatic gel mobility shift of Cdc25C has long been used as an experimental marker for Cdc25C activation during G2/M transition, and much effort has been directed toward identifying the kinase

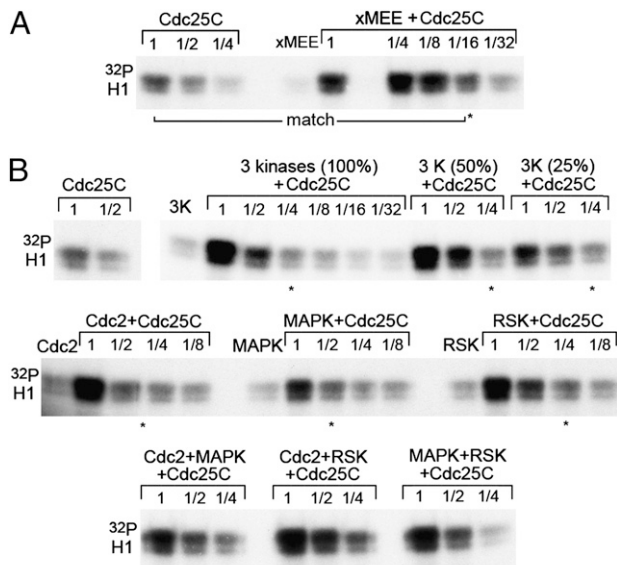


**Fig. 6.** MAPK, Cdc2, and RSK2 together do not fully activate GST-Cdc25C. (A) The latent Cdc2/cyclin B complex was treated with indicated dilutions of nonphosphorylated or 1:4 MEE-phosphorylated GST-Cdc25C and then measured for phosphorylation of histone H1 by <sup>32</sup>P incorporation. (B) The latent Cdc2/cyclin B complex was treated with GST-Cdc25C that had been phosphorylated by indicated combinations of Cdc2, MAPK, and RSK2 and then measured for phosphorylation of histone H1 by <sup>32</sup>P incorporation. Active Cdc2, MAPK, and RSK2 were partially purified from MEE and were used at two- to fourfold higher levels than their levels in 1:4 MEE.

(s) that induces this shift. However, although phosphorylation of GST-Cdc25C with *Xenopus* egg extracts recapitulates the dramatic gel mobility shift of Cdc25C, none of the purified GST-Cdc25C-activating kinases from *Xenopus* egg extracts induces a substantial mobility shift in GST-Cdc25C. The repeated “failure” predicts that the shift-inducing kinase either is highly unstable or requires preexisting conditions for phosphorylation of Cdc25C. Our previous results showed that phospho-defective mutations of the three identified MAPK sites T48-T138-S205 in myc-Cdc25C quantitatively eliminate the dramatic gel mobility shift of Cdc25C during progesterone-induced *Xenopus* oocyte maturation although MAPK-catalyzed phosphorylation is unable to directly induce a dramatic gel mobility shift in GST-Cdc25C (13). Moreover, the phospho-defective mutation of the MAPK site T48 in GST-Cdc25C<sub>9-129</sub> eliminates its dramatic gel mobility shift in MEE although the T48 phosphorylation induces only a slight gel mobility shift in GST-Cdc25C<sub>9-129</sub> (14). These findings certainly support the second possibility and suggest a model whereby full activation of Cdc25C involves the mechanistically distinct priming phosphorylation and secondary phosphorylation steps. If this two-step activation model is correct, MAPK, Cdc2, and RSK each may be able to both partially activate Cdc25C and generate primed Cdc25C for the secondary phosphorylation and full activation during *Xenopus* oocyte maturation. Apparently, testing this framework of thinking requires a different set of experiments, including characterization of the prerequisite(s), the chemical basis, and the responsible kinase(s) for the big shift-producing secondary phosphorylations of Cdc25C and examination of their functional impact on Cdc25C activation.

## Materials and Methods

**Preparation and Fractionation of *Xenopus* Egg Extracts, Immunoblotting, and Immunodepletion.** Preparation and biochemical fractionation of *Xenopus* egg extracts and antibodies used in this study are described in *SI Materials and Methods*. Immunoblotting, immunodepletion, and p13-based Cdc2 absorp-

tion were performed with procedures described in our previous publications (9, 13, 24).

### Phosphorylation of GST-Tagged Cdc25C Proteins and Assays of Cdc25C Activity.

Bacterial expression vectors for GST-tagged Cdc25C proteins and CA-RSK and identification of phosphorylated amino acids by mass spectrometry are described in *SI Materials and Methods*. Vectors, templates and PCR primers used in producing new expression constructs are described in Table S1. Production of purified GST-tagged Cdc25C proteins, preparation of activated recombinant p42 MAPK, in vitro phosphorylation of GST-tagged Cdc25C proteins, and measurement of the phosphatase activity of His-Cdc25C- or Cdc2/cyclin B-activating activity of GST-Cdc25C were performed as previously described (13).

**Injection and Maturation of *Xenopus* Oocytes.** Stage VI *Xenopus* oocytes were obtained, microinjected, matured with progesterone (Sigma), observed for germinal vesicle breakdown (morphological indicator of oocyte maturation), and extracted as previously described (13). Okadaic acid (OA) was not included in the oocyte extraction buffer when the Cdc25C phosphorylation at 317–319 was examined because OA sometimes induced the phosphorylation of Cdc25C at 317–319 in immature oocyte extracts. A total of 50 μM of the MEK1 inhibitor U0126 (Calbiochem) or 4 mM of the RSK inhibitor SL0101 (Toronto Research Chemicals) was added to oocyte culture medium 30 min before progesterone stimulation or mRNA injection. These concentrations of the inhibitors were used in previous studies (25). Production of mRNAs for oocyte injection are described in *SI Materials and Methods*.

**ACKNOWLEDGMENTS.** We thank Cheryl A. Ashorn and Mayra Nelman-Gonzalez for providing technical assistance. This work was supported by National Institutes of Health/National Cancer Institute Grant R01 CA93941 and DOD Grant W81XWH-08-PCRP-SIDA (to J.K.) and by U54 Grant CA090810 and P20 Grant CA101936 (to G.E.G.). M phase-arrested *Xenopus* egg extracts were prepared by Dr. Marc Kirchner's laboratory (Harvard Medical School). Protein identification by mass spectrometry was performed by the Proteomics Core Facility of the University of Texas M. D. Anderson Cancer Center. DNA sequencing was performed by the DNA Analysis Facility of the University of Texas M. D. Anderson Cancer Center supported by National Cancer Institute Grant CA-16672.

- Morgan DO (1997) Cyclin-dependent kinases: Engines, clocks, and microprocessors. *Annu Rev Cell Dev Biol* 13:261–291.
- Nurse P (1996–1997) The central role of a CDK in controlling the fission yeast cell cycle. *Harvey Lect* 92:55–64.
- Izumi T, Walker DH, Maller JL (1992) Periodic changes in phosphorylation of the *Xenopus* cdc25 phosphatase regulate its activity. *Mol Biol Cell* 3:927–939.
- Jessus C, Beach D (1992) Oscillation of MPF is accompanied by periodic association between cdc25 and cdc2-cyclin B. *Cell* 68:323–332.
- Kumagai A, Dunphy WG (1992) Regulation of the cdc25 protein during the cell cycle in *Xenopus* extracts. *Cell* 70:139–151.
- Alberts B, et al. (2002) The activation of M-phase cyclin-Cdk complexes (M-Cdks) triggers entry into mitosis. *Molecular Biology of the Cell*, ed Alberts B (Garland Science, New York), 4th Ed, pp. 999–1000.
- Ferrell JE, Jr. (1999) *Xenopus* oocyte maturation: New lessons from a good egg. *Bioessays* 21:833–842.
- Masui Y, Markert CL (1971) Cytoplasmic control of nuclear behavior during meiotic maturation of frog oocytes. *J Exp Zool* 177:129–145.
- Kuang J, et al. (1991) Multiple forms of maturation-promoting factor in unfertilized *Xenopus* eggs. *Proc Natl Acad Sci USA* 88:11530–11534.
- Karaiskou A, Cayla X, Haccard O, Jessus C, Ozon R (1998) MPF amplification in *Xenopus* oocyte extracts depends on a two-step activation of cdc25 phosphatase. *Exp Cell Res* 244:491–500.
- Wu M, Gerhart JC (1980) Partial purification and characterization of the maturation-promoting factor from eggs of *Xenopus laevis*. *Dev Biol* 79:455–457.
- Izumi T, Maller JL (1995) Phosphorylation and activation of the *Xenopus* Cdc25 phosphatase in the absence of Cdc2 and Cdk2 kinase activity. *Mol Biol Cell* 6:215–226.
- Wang R, et al. (2007) Regulation of Cdc25C by ERK-MAP kinases during the G2/M transition. *Cell* 128:1119–1132.
- Wu CF, et al. (2010) Dissecting the M phase-specific phosphorylation of serine-proline or threonine-proline motifs. *Mol Biol Cell* 21:1470–1481.
- Leighton IA, Dalby KN, Caudwell FB, Cohen PT, Cohen P (1995) Comparison of the specificities of p70 S6 kinase and MAPKAP kinase-1 identifies a relatively specific substrate for p70 S6 kinase: The N-terminal kinase domain of MAPKAP kinase-1 is essential for peptide phosphorylation. *FEBS Lett* 375:289–293.
- Chun J, et al. (2005) Phosphorylation of Cdc25C by pp90Rsk contributes to a G2 cell cycle arrest in *Xenopus* cycling egg extracts. *Cell Cycle* 4:148–154.
- Anjum R, Roux PP, Ballif BA, Gygi SP, Blenis J (2005) The tumor suppressor DAP kinase is a target of RSK-mediated survival signaling. *Curr Biol* 15:1762–1767.
- Roux PP, Ballif BA, Anjum R, Gygi SP, Blenis J (2004) Tumor-promoting phorbol esters and activated Ras inactivate the tuberous sclerosis tumor suppressor complex via p90 ribosomal S6 kinase. *Proc Natl Acad Sci USA* 101:13489–13494.
- Gottlin EB, et al. (1996) Kinetic analysis of the catalytic domain of human cdc25B. *J Biol Chem* 271:27445–27449.
- Richards SA, Dreisbach VC, Murphy LO, Blenis J (2001) Characterization of regulatory events associated with membrane targeting of p90 ribosomal S6 kinase 1. *Mol Cell Biol* 21:7470–7480.
- Gross SD, Lewellyn AL, Maller JL (2001) A constitutively active form of the protein kinase p90Rsk1 is sufficient to trigger the G2/M transition in *Xenopus* oocytes. *J Biol Chem* 276:46099–46103.
- Haccard O, Lewellyn A, Hartley RS, Erikson E, Maller JL (1995) Induction of *Xenopus* oocyte meiotic maturation by MAP kinase. *Dev Biol* 168:677–682.
- Haccard O, Jessus C (2006) Redundant pathways for Cdc2 activation in *Xenopus* oocyte: either cyclin B or Mos synthesis. *EMBO Rep* 7:321–325.
- Kuang J, Ashorn CL (1993) At least two kinases phosphorylate the MPM-2 epitope during *Xenopus* oocyte maturation. *J Cell Biol* 123:859–868.
- Inoue D, Ohe M, Kanemori Y, Nobui T, Sagata N (2007) A direct link of the Mos-MAPK pathway to Erp1/Emi2 in meiotic arrest of *Xenopus laevis* eggs. *Nature* 446:1100–1104.